from the following equation:[16]

$$\Delta E=\frac{13.56}{K^2}\frac{m_p}{m}\text{ev} \tag{11}$$

that the effective mass for holes is about $0.35m$. These values thus are in fairly good agreement. Since we have not made n-type gallium antimonide, no independent evaluation of the effective mass of electrons is available in our work.

SUMMARY AND CONCLUSIONS

Single crystals of gallium antimonide have been prepared, and their properties have been determined over a wide range of temperature. These properties have been found to fit well with the present theory of semiconductors. Of special interest among the results are the large ratio of electron to hole mobility (about five), the rather large intrinsic band gap (0.8 ev). Also, it is necessary to assume two acceptor levels in the energy scheme to fit the Hall data. A value of the hole effective mass has been estimated from the infrared absorption data, and from the electrical properties.

[16] See reference 12, p 224.

ACKNOWLEDGMENTS

We should like to thank Dr. R. Newman for the use of his infrared absorption data, and for fruitful discussions. We should also like to thank Dr. W. W. Tyler for growing the single crystals.

PHYSICAL REVIEW VOLUME 95, NUMBER 1 JULY 1, 1954

Theory of Secondary Electron Cascade in Metals

P. A. WOLFF
Bell Telephone Laboratories, Murray Hill, New Jersey
(Received March 5, 1954)

A study is made of the cascade process which describes the diffusion, energy loss, and multiplication of secondary electrons within a metal. The secondaries interact mainly with conduction electrons through a screened Coulomb potential. For low secondary energy (<50 ev) the resultant scattering is nearly spherically symmetric and the transport equation which governs the cascade process can be approximately solved. The velocity distribution turns out to be spherically symmetric for low secondary energy. Energy distributions are in agreement with experiment for metals to which the theory is applicable. Calculations are also made of the rate of change of yield with work function and the results are in accord with observed values. Finally, rough estimates are made of the total yield and the theory is shown to be consistent with the observed values.

I

THE phenomenon of secondary electron emission[1] can be thought of as occurring in two distinct steps. First of these is the production of internal secondaries by collisions between fast primaries and electrons bound in the metal. The second is the subsequent cascade process in which these secondaries diffuse through the solid, multiplying and losing energy en route, until they either sink back into the sea of conduction electrons or reach the surface with sufficient energy to emerge as true secondary electrons. These two steps pose two separate problems, each of considerable complexity, which must be solved before one can understand the various phases of SE. To date, most of the theoretical work[2] in the field has concentrated on the first of these and treated the second in a radically simplified way. Usually the whole second step is lumped into an effective absorption coefficient α for the internal secondaries. Calculations using this approach have given fair agreement with the shapes of observed total yield *versus* primary energy curves, but they cannot predict the absolute magnitude of the yield since, without solving the diffusion problem, there is no way of estimating α.

Other aspects of SE probably depend even more critically on the details of the internal electron cascade. For example, the energy distribution of secondaries is observed to be independent of primary voltage. This suggests that the cascade process is almost entirely responsible for the shape of the spectrum and that the method of production of the internal secondaries is relatively unimportant. The aim of the present work is to investigate this internal electron cascade and to verify to what extent this hypothesis is correct. The picture of SE which will arise from this study turns out to be a reasonable and consistent one which accounts for a number of the experimental results.

To solve the problem of the internal cascade one must, of course, know the elementary interactions by which electrons lose energy within the metal. This

[1] Hereafter abbreviated as SE.

[2] For a review and bibliography of work performed prior to 1948 see K. G. McKay's article in *Advances in Electronics* (Academic Press, Inc., New York, 1948). Other, more recent, articles are E. M. Baroody, Phys. Rev. **78**, 780 (1950); A. J. Dekker and A. van der Ziel, Phys. Rev. **86**, 755 (1952); J. F. Marshall, Phys. Rev. **88**, 416 (1952).

subject, which is clearly a critical one in the theory, will be discussed in the next section. Following that, the remainder of the paper will be devoted to a study of the transport equation whose solution provides the energy distribution of secondaries. Various methods of attacking this problem will be investigated and, finally, a comparison will be made between theory and the results obtained experimentally.

II

For an electron to escape from a metal and be observed as a secondary it must have an energy of about ten volts or more relative to the bottom of the conduction band.[3] In this energy range, where the exclusion principle does not operate strongly, the main way it loses energy is by collision with conduction electrons in the metal. Electron-phonon interactions also undoubtedly occur, but the fact that SE from metals is independent of temperature indicates that they play only a minor role in the slowing down process. They will be neglected here and only electron-electron collisions considered in calculating energy loss. Furthermore, in discussing these collision processes the electrons will be treated as free; no attempt will be made to include the effect of the crystal field on the scattering. The validity of this approximation depends to a large extent upon the material being studied, but for simple, monovalent metals such as the alkalis and noble metals it probably is reasonably close to the truth.

The potential U which causes electron-electron scatterings is the Coulomb field, screened by the plasma of conduction electrons. Probably the best calculation of the effect of the screening is that of Pines and Bohm[4] who found

$$U=\sum_{\mathbf{k},k<k_c}\left[\frac{4\pi e^2 e^{i\mathbf{k}\cdot\mathbf{r}}}{k^2}\right]. \tag{1}$$

Other potentials have also been used. For example, Mott[5] in his paper on impurity scattering employs a screened potential of the form

$$U=e^2e^{-qr}/r, \tag{2}$$

where

$$q=\frac{4me^2}{\hbar^2}\left(\frac{3p_0}{\pi}\right)^{\frac{1}{3}}. \tag{3}$$

Fortunately, for the present purpose the form of U is rather unimportant. The crucial point is that in all these potentials the cut-off distance is small; for a typical metal the values of k_c used by Pines[6] correspond to lengths of about 1A and the $1/q$ values used by Mott are considerably smaller. With such short range potentials the scattering is spherically symmetric (s wave) over a considerable range of electron energies. By way of illustrating this point, Table I gives the s- and p-wave phase shifts for an $(e^2/r)\exp(-r/\lambda_D)$ potential, with λ_D taken as 0.75A and 1.00A. These values were obtained by numerically integrating the appropriate Schrödinger equation; from them it is clear that s-wave scattering predominates for low energies and that even at 50 ev it constitutes about one-half of the total scattering cross section. Below 50 ev, therefore, the scattering is roughly spherically symmetric (in the center of mass system) which means that, on the average, an electron loses about half its energy at each collision. This is in marked contrast to the behavior of faster electrons which suffer typical Rutherford scattering and lose only a small fraction of their energy at each impact. In solving the transport equation, therefore, the correct electron-electron cross section to use is one that is spherically symmetric for small electron energy but which develops more and more of a forward peak as the energy increases, eventually approaching the Coulomb cross section. Unfortunately, with such a general interaction the transport equation, which gives the spatial and energy distributions of internal secondaries, is far too difficult to solve. Therefore, in order to get at least a semiquantitative idea of how these internal electrons behave, the electron-electron scattering will be assumed to be spherically symmetric up to an energy W (about 100 ev), beyond which it will be described by Rutherford's formula. This is a very rough approximation but, fortunately, it should not have a great effect on the shapes of the SE spectra, since they are almost entirely determined by the behavior of electrons with energies below about 40 ev. As a consequence of this fact, the spectra also turn out to be quite insensitive to the choice of W. The value of 100 ev given above is hardly more than an intelligent guess based on experience gained in evaluating the phase shifts for the screened Coulomb field, but a variation in it by 50 percent in either direction would only change the energy distribution by a few percent in the low-energy region. Thus, even with the crude approximation outlined above, the theoretical spectra should be fairly accurate in the 0–40 ev range where most of the secondaries fall. For higher energies,

TABLE I. Phase shifts for scattering from screened Coulomb potential.

E (Rydbergs)	δ_0(s-wave phase shift)	δ_1(p-wave phase shift)
	$\lambda_D=0.75$A	
2	−24°	−1° 20′
4	−24° 40′	−5° 40′
6	−25°	−5° 40′
	$\lambda_D=1.00$A	
2	−31°	−8° 30′
4	−32°	−9°

[3] In this paper all energies will be measured from the bottom of the conduction band.
[4] D. Pines and D. Bohm, Phys. Rev. **85**, 338 (1952).
[5] N. F. Mott, Proc. Cambridge Phil. Soc. **32**, 281 (1936).
[6] David Pines (private communication).

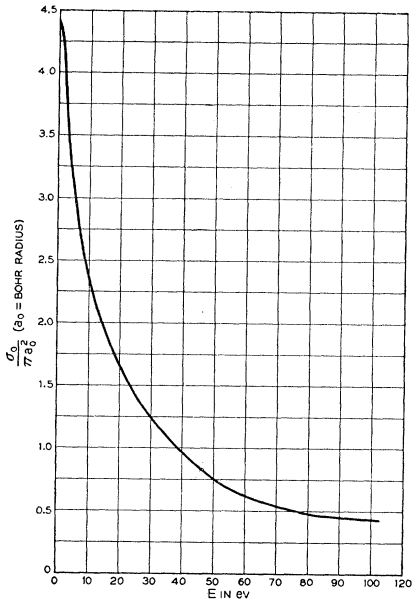

FIG. 1. Electron scattering cross section *versus* electron energy.

of course, the formulas are much less reliable and could give large errors in the number of secondaries.

For low electron energy, the numerical value of the electron-electron cross section is given by the usual formula[7]

$$\sigma=(4\pi/k^2)\sin^2\delta_0,$$

where the values of δ_0 are taken from Table I. Figure 1 shows the σ *vs* E curve obtained in this manner using a cut-off distance of 0.75A. Of course, this cross section still has to be corrected for the effect of the exclusion principle since scatterings in which either of the electrons winds up with energy less than the Fermi energy are forbidden. For the time being, however, this point will be neglected; it will be considered in detail at a more convenient point in the later discussion of the transport equation.

III

The equation describing the electron cascade process within the metal is the same as that given by Marshak[8] for neutron slowing down, namely,

$$\frac{\partial N}{\partial t}(\mathbf{r},\boldsymbol{\Omega},E,t)+\mathbf{v}\cdot\mathrm{grad}N(\mathbf{r},\boldsymbol{\Omega},E,t)$$
$$=-\frac{vN(\mathbf{r},\boldsymbol{\Omega},E,t)}{l(E)}+S(\mathbf{r},\boldsymbol{\Omega},E,t)+\int dE'$$
$$\times\int\frac{d\Omega' v' N(\mathbf{r},\boldsymbol{\Omega}',E',t)}{l(E')}F(\boldsymbol{\Omega},E;\boldsymbol{\Omega}'E'). \quad (5)$$

[7] See, for example, N. F. Mott and H. S. W. Massey, *Theory of Atomic Collisions* (Oxford Press, London, 1933).
[8] R. E. Marshak, Revs. Modern Phys. **19**, 185 (1947).

Here $N(\mathbf{r},\boldsymbol{\Omega},E,t)$ is the number of electrons between $\mathbf{r}$ and $\mathbf{r}+d\mathbf{r}$, $\boldsymbol{\Omega}$ and $\boldsymbol{\Omega}+d\boldsymbol{\Omega}$, E and $E+dE$ at time t, where $\mathbf{r}$ represents space coordinates, $\boldsymbol{\Omega}$ is a unit vector in the direction of the electron velocity, $\mathbf{v}$ is the electron velocity, and E the energy. $l(E)$ is the mean free path and $F(\boldsymbol{\Omega},E;\boldsymbol{\Omega}'E')$ the probability that, given an electron at $\boldsymbol{\Omega}'E'$, one will be found at $\boldsymbol{\Omega}$, E after a scattering. $S(\mathbf{r},\boldsymbol{\Omega},E,t)$ is a source term representing the density of internal secondaries produced by the primary bombardment. It should be emphasized that the factor $F(\boldsymbol{\Omega},E;\boldsymbol{\Omega}'E')$ takes into account two types of electrons: those which scatter down in energy from $\boldsymbol{\Omega}'$, E' to $\boldsymbol{\Omega}$, E; and those which are knocked up from the conduction band to $\boldsymbol{\Omega}$, E. Thus, this term specifically includes the electron multiplication and is not normalized to unity as in Marshak's paper. Indeed, if the effect of the exclusion principle on the scattering is neglected, the correct normalization factor is twice his

$$\int_0^{E'}dE\int d\Omega(F(\boldsymbol{\Omega},E;\boldsymbol{\Omega}',E')=2. \quad (6)$$

This equation expresses the fact that for each electron in the cascade which scatters, there are two present after the collision.

The most common geometry in SE experiments is one in which the primary electrons are incident normally on a plane surface. With this configuration the problem is one-dimensional and has azimuthal symmetry, which means that Eq. (5) simplifies greatly. For the steady state ($\partial N/\partial t=0$) it contains three variables; z, the distance normal to the surface; θ, the angle that the velocity of the secondary electron makes with the normal; and the energy E. Following the usual procedure (see Marshak's paper, for example) N, F, and S are expanded into spherical harmonics

$$N(z,\cos\theta,E)=(1/4\pi)\textstyle\sum_l(2l+1)N_l(z,E)P_l(\cos\theta),$$
$$S(z,\cos\theta,E)=(1/4\pi)\textstyle\sum_l(2l+1)S_l(z,E)P_l(\cos\theta),$$
$$F(\boldsymbol{\Omega},E;\boldsymbol{\Omega}'E')=F(\cos\Theta;E,E') \quad (7)$$
$$=(1/4\pi)\textstyle\sum_l(2l+1)F_l(E,E')P_l(\cos\Theta),$$

where Θ is the angle between the vectors $\boldsymbol{\Omega}'$ and $\boldsymbol{\Omega}$. With the abbreviation $\psi_l=vN_l/l(E)$ the following set of simultaneous integro-differential equations in z and E is obtained

$$\psi_l=l(E)\left[\left(\frac{l}{2l+1}\right)\frac{\partial\psi_{l-1}}{\partial z}+\left(\frac{l+1}{2l+1}\right)\frac{\partial\psi_{l+1}}{\partial z}\right]$$
$$+\int_E^\infty dE'F_l(E,E')\psi_l(z,E')+S_l(z,E). \quad (8)$$

These are the equations which govern the cascade process for the simple geometry under consideration. Most of the remainder of this article will be devoted to various approximate ways of solving them.

Since Eqs. (8) are quite complicated it is important to examine them in various special cases. One of great interest is that in which ψ_l is independent of z. This corresponds to a situation in which the internal secondaries are produced uniformly deep inside a metal (away from the influence of the surface). Although this is rather a far cry from the usual experimental situation in which secondaries are observed as they leave the surface, the fact that observed secondary electron spectra are almost entirely independent of primary energy suggests that the depth of penetration of the primaries (and hence the distance the cascade develops from the surface) is relatively unimportant and that calculations of this type may give reasonably good expressions for the energy distributions. This expectation is actually borne out by later work which correctly includes the space variation for a particular choice of F in Eq. (5). For the time being, therefore, consider the case in which ψ_l is independent of z. Equations (8) then reduce to a set of uncoupled integral equations,

$$\psi_l=\int_E^\infty dE' F_l(E,E')\psi_l(E')+S_l(E). \tag{9}$$

These will be solved first with a simplified expression for $F_l(E,E')$. The results of this calculation will then be used as a guide in treating the problem with a more realistic choice of F_l. F_l is determined by inverting Eq. (7)

$$F_l(E,E')=\int d\Omega F(\cos\Theta;E,E')P_l(\cos\Theta). \tag{10}$$

In line with the arguments of Sec. II, F is taken to be spherically symmetric. The simplification mentioned above comes in also assuming that the conduction electrons are moving slowly compared to those in the cascade. This means that the energy of an electron after scattering is determined uniquely by the scattering angle and its initial energy (hence the delta function in the formula below). Under these conditions F is given by

$$F(\cos\Theta;E,E')=\frac{2}{4\pi}\delta[E-E'\cos^2\Theta]4\cos\Theta, \tag{11}$$

where the factor $4\cos\Theta$ is the Jacobian of the transformation from center of mass to laboratory angles.

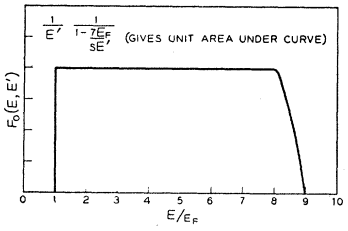

FIG. 2. $F_0(E,E')$ *versus* E/E_F for $E'=9E_F$.

$F_l(E,E')$ can now be obtained from Eq. (10),

$$F_l(E,E')=\frac{2}{E'}P_l\left(\sqrt{\frac{E}{E'}}\right). \tag{12}$$

The factor two which appears here takes care of the electron multiplication and is the same as that appearing in the normalization of F [Eq. (6)]. The integral equations now read

$$\psi_l=2\int\frac{dE'}{E'}P_l\left(\sqrt{\frac{E}{E'}}\right)\psi_l(E')+S_l(E). \tag{13}$$

The homogeneous equations have solutions of the form

$$\psi_l\sim E^{\alpha_l}, \tag{14}$$

where the values of α_l are obtained from the formula

$$1=2\int_1^\infty x^{(\alpha_l-1)}P_l\left(\sqrt{\frac{1}{x}}\right)dx. \tag{15}$$

For the first three spherical harmonics the α_l's turn out to be $\alpha_0=-2$, $\alpha_1=-\frac{3}{2}$, $\alpha_2=-\frac{1}{2}\pm\frac{1}{2}i\sqrt{3}$. With these functions the complete solution of Eq. (13) is obtained by integrating over S_l. It is readily verified (by substitution) that ψ_l is given by

$$\psi_l=-\int_E^\infty\left(\frac{E}{E'}\right)^{\alpha_l}\frac{\partial S_l}{\partial E'}dE'. \tag{16}$$

Electron multiplication clearly plays an important role in determining the α_l values given above. Neglecting it [by replacing the factor two in Eq. (13) by unity] gives, for example, $\alpha_0=-1$ instead of -2. Thus, it strongly emphasizes the singularity at zero in the energy distribution. Another important feature is also apparent from these figures; namely that in going towards larger l values the order of the singularity at zero energy decreases rapidly. Physically this is very reasonable since a high spherical harmonic represents a complicated and special angular distribution which is easily smeared out by scattering. The net effect is that at low energies the internal electron velocity distribution is nearly spherically symmetric since the electrons have made enough collisions to wash out any angular variation. Of course, this argument is hardly correct for the p wave ($l=1$), but it will not be highly excited in any case since the secondaries are mainly produced at right angles to the primary beam which means a small $P_1(\cos\theta)$ component in S.

The above conclusions have been obtained by using a special form for $F(\Omega,E;\Omega,E')$, a form which gives a unique relation between E, E', and cos. In the actual case the formula

$$E=E'\cos^2\Theta \tag{17}$$

will only give the average energy after a scattering—there will always be a spread around this value because

interactions are not with stationary particles (as was assumed previously) but with moving conduction electrons. This effect strengthens the conclusion that for small energies the electron distribution is spherically symmetric. It furnishes another source of averaging so that angular variations are wiped out even sooner than the values of α_l given above suggest. Thus, the high harmonics are only important for large E and are soon overwhelmed by ψ_0, which grows very rapidly as $E\to 0$ and determines the shape of the energy distribution. For this reason, attempts to improve the approximate solutions discussed above will concentrate on the spherically symmetric part of ψ.

IV

The expression for ψ_0 given in the previous section [Eq. (14)] is inaccurate because the F_0 used in the integral equation takes no account of either the exclusion principle or motion of the conduction electrons. The correct F_0 is given by

$$F_0=\int d\Omega F(\cos\Theta; E,E') \tag{18}$$

and is just the total probability of scattering from energy E' to E, irrespective of angle. For S-wave scattering from a degenerate Fermi gas this quantity has been evaluated by Goldberger.[9] An examination of his analysis shows that F_0 is unaffected by the motion of the electrons, but is changed through the exclusion principle. The resultant F_0, instead of being flat as a function of E, has the form shown in Fig. 2. The differences between this curve and the previous F_0 have a clear physical interpretation. Below $E=E_F$ (E_F=Fermi energy) there is a gap because no electron may wind up with less energy than E_F. For $E'>E>E'-E_F$ the curve tails off because collisions are impossible unless the target electron is within $E'-E$ of the surface of the Fermi sphere. Within this range, therefore, the number of conduction electrons available for scattering is decreasing, approaching zero at $E=E'$.

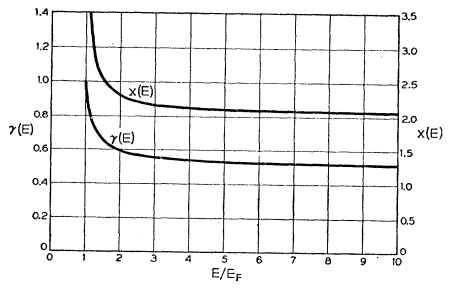

FIG. 3. $\gamma(E)$ and $x(E)$ *versus* E.

[9] M. L. Goldberger, Phys. Rev. **74**, 1269 (1948). Goldberger's calculation is made for a cross section which is constant in energy. This is not strictly true in the present case, but the variation of σ is slow enough that his formula is a good approximation.

Besides changing F_0, the exclusion principle reduces the total scattering cross section. This effect has also been considered by Goldberger who finds

$$\sigma_{\text{eff}}=\sigma_0(1-7E_F/5E), \tag{19}$$

where this formula, as well as the curve given for F_0, are valid for $E>2E_F$. This gives a mean free path

$$l(E)=\frac{1}{n_c\sigma_0(E)(1-7E_F/5E)} \tag{20}$$

to be used in calculating N_0 from ψ_0. In this formula the energy dependence of the two factors, $\sigma_0(E)$ and $(1-7E_F/5E)$, is in the opposite sense so that the mean free path is roughly constant (to within 25 percent) over the energy range 10–50 ev.

With the new $F_0(E,E')$ the integral equation [Eq. (13)] is no longer solved by a ψ_0 which is a simple power of E. As is clear from Fig. 2, the main effect of the exclusion principle on F_0 is to increase the average energy after scattering. This can be expressed by writing

$$\bar{E}=\alpha(E')E', \tag{21}$$

where E' is the energy before scattering, $\bar{E}$ the average energy afterwards, and $\alpha(E')=\frac{1}{2}$ for $E/E_F\ll 1$, but gradually rises as E' decreases. A rough idea of how this effect influences the energy distribution can be gained by assuming that the energy after collision is always given by the average energy of Eq. (21). This method gives the correct $1/E^2$ distribution for large E, and will also be right for small $E(E\sim E_F)$ since there, because of the exclusion principle, the energy spread around $\bar{E}$ is small. This method should, therefore, give a satisfactory interpolation between high and low E. With it the integral equation reads

$$\psi_0(E)=2\int\delta[E-E'\alpha(E')]\psi_0(E')dE'. \tag{22}$$

Since there is a one-to-one relation between $\bar{E}$ and E' (according to Eq. (21)) one can also write

$$\bar{E}=\gamma(\bar{E})E'. \tag{23}$$

The integral in Eq. (22) can now be performed directly, giving

$$\psi_0(E)=\frac{2}{\gamma(E)}\psi_0\left[\frac{E}{\gamma(E)}\right]. \tag{24}$$

This equation has a solution of the form $\psi\sim 1/E^x$, where

$$2[\gamma(E)]^{x-1}=1. \tag{25}$$

In Fig. 3, $\gamma(E)$ and $x(E)$ are plotted as functions of E. As expected, $x(E)$ has the value two for large E and rises slowly as the energy gets smaller. At $E=2E_F$, which is where the energy spectrum begins to be dominated by the effect of the escape probability

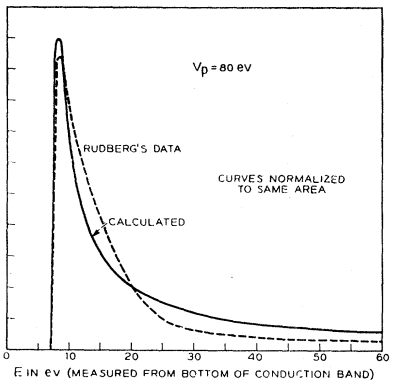

FIG. 4. Energy distribution of secondary electrons from Li.

[$P(E)$ of Eq. (27)], $x(E)$ has only reached 2.3. Thus, the effect of exclusion on F_0 does not change the spectrum greatly and this rough way of taking it into account is probably adequate. Using this approximation, the current is given by

$$j=Nv=\frac{\psi_0}{l(E)}=P(E)\frac{1}{n_c\sigma_0(E)(1-7E_F/5E)}\left(\frac{E_0}{E}\right)^x. \quad (26)$$

Here $x(E)$ is taken from Fig. 2, and $P(E)$ is a geometrical factor which gives the probability that an electron with energy E that strikes the surface will have a large enough normal velocity to overcome the work function and escape. For a spherically symmetric distribution, $P(E)$ is given by

$$P(E)=1-[(\varphi+E_F)/E]^{\frac{1}{2}}, \quad (27)$$

where φ is the work function.

V

According to the assumption of Sec. II, Eq. (26) is valid when $E_0<W$. Therefore, when the primary electron energy is less than 100 ev the spectrum of secondaries can be obtained directly from Eq. (26) by replacing E_0 by V_p. A simple metal that has been studied for bombarding energies in this range is lithium, which was investigated by Rudberg.[10] In Fig. 4 a comparison is made between theory and his results in this case. Of particular interest is the fact that both the theoretical and experimental spectra have very small half-widths—widths which are smaller by a factor of three than those observed in Au or Ag. This happens because the work function of Li is smaller, in comparison to its Fermi energy, than those of Au or Ag. Therefore, in units of E_F, the vacuum level in lithium lies considerably closer to the Fermi level than it does in the other two metals. Near the Fermi level, however, the internal energy distribution is falling steeply from the infinity at $E=E_F$. The external distribution, which is a product of the internal distribution and the escape probability of Eq. (27), is therefore quite narrow since the rapidly falling internal distribution cuts off the spectrum very sharply on the high energy side. For Au or Ag, on the other hand, the work function is considerably larger and the SE spectra are placed higher relative to E_F. The part of the internal distribution which determines the spectrum is, therefore, much flatter than for Li which means a broader and smoother energy distribution.

For bombarding energies greater than W, Eq. (26) cannot be used as simply as above. Electrons with energy greater than W must be followed individually, their rate of energy loss and secondary production being calculated from Rutherford's formula, until they reach energy W where they can be described by Eq. (26). These fast electrons produce secondaries, by small-angle Coulomb scattering, which are distributed in energy according to a $1/E^2$ law. For $E_0<W$, this distribution function can be used directly in Eq. (16). In addition, there are also a few secondaries produced with energy greater than W. For the bombarding energy of 155 ev used by Rudberg[11] on Cu, Ag, and Au they are quite few in number, however, and can be neglected in analyzing his data. Thus, of the 155-ev primary energy, 55 ev goes into a $1/E_0^2$ energy distribution extending up to W and the rest is accounted for by the fast electron which ultimately winds up with 100 ev and there joins the cascade described by Eq. (26). The complete source distribution to be used in the integral of Eq. (16) therefore consists of one electron with energy W plus a $1/E_0^2$ distribution containing the rest of the primary energy. This source function turns out to be $S=(0.1W/E_0^2)+\delta(W-E_0)$ if the maximum impact parameter, which determines the minimum value of E_0, is taken equal to the screening radius. In Fig. 5 the theoretical curve obtained using it is plotted along with Rudberg's data on silver. As in the case of Li, the theoretical curve is somewhat sharper than the experimental. However, the overall agreement is good and, in

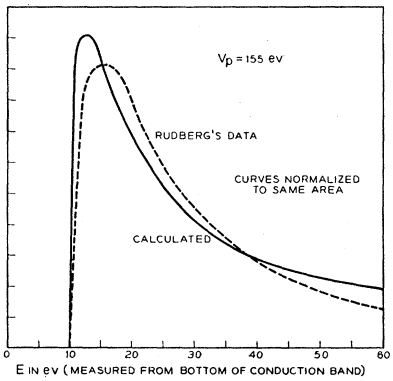

FIG. 5. Energy distribution of secondary electrons from Ag.

[10] Erik Rudberg, Kgl. Svenska Vetenskapsakad. Handl. No. **7**, (1929).

[11] Erik Rudberg, Phys. Rev. **50**, 138 (1936).

particular, the half-width is correct to about 15 percent. As one would expect from examining the φ and E_F values for Ag and Au, the spectrum obtained from gold is almost identical to that from silver. In copper the φ/E_F ratio is smaller than for Au or Ag, which explains the fact that it has a somewhat narrower energy distribution than the other two metals.

When the energy of bombarding electrons is appreciably larger than W, the above treatment must be modified to take account of the secondaries produced with energies greater than W. However, the argument given in Sec. II indicates that for low electron energy the shape of the SE spectrum should be relatively unaltered since it is mainly determined by the behavior of electrons at energies near or below about 50 ev. Thus, one would expect to obtain energy distributions like those in Figs. 4 and 5 for all values of the primary energy.

VI

In the two previous sections Eq. (5) was solved under the assumption that N was independent of z. An argument based on the fact that electron spectra are independent of primary energy was then used to suggest that this solution corresponds closely to the observed energy distribution. That this is actually the case will be demonstrated by solving Eq. (5), including the space variation of N, for the geometry discussed in Sec. III.

For this geometry the surface of the metal is taken to be the plane $z=0$ and the source function is chosen as

$$\begin{aligned} &S_l=0 && (l\neq 0),\\ &S_0=A\delta(E-E_0) && z>0,\\ &S_0=0 && z<0. \end{aligned} \tag{29}$$

This is a reasonable choice for S_l provided the primary electrons are fast enough not to lose an appreciable fraction of their energy in a distance equal to the range of a typical secondary. With this S, the transport problem becomes almost identical with one solved by Weymouth.[12] His method consists in neglecting all but the first two spherical harmonics in the expansion of N. The result is a pair of simultaneous integro-differential equations. For a constant mean free path $[l(E)=l_0]$ and the F_l's given in Eq. (12), they are

$$\begin{aligned} &l_0\frac{\partial\psi_1}{\partial z}+\psi_0=2\int\psi_0(E')\frac{dE'}{E'}+S_0(z,E),\\ &\frac{l_0}{3}\frac{\partial\psi_0}{\partial z}+\psi_1=2\int\left(\frac{E}{E'}\right)^{\frac{1}{2}}\psi_1(E')\frac{dE'}{E'}. \end{aligned} \tag{30}$$

The solutions of these equations can be obtained by using Weymouth's analysis. This is a purely mathematical problem, however, and will not be treated in detail here; a brief outline of the procedure is given in Appendix A. The result of these calculations is that $\psi_0(0,E)$ and $\psi_1(0,E)$ turn out to have an energy dependence given by the series

$$\frac{1}{E}\left[0.54+0.48\mu+\frac{0.46\mu^2}{2!}+\frac{0.46\mu^3}{3!}+\frac{0.43\mu^4}{4!}+\cdots\right], \tag{31}$$

where $\mu=\ln(E_0/E)$. This series approximates closely to

$$\frac{0.50}{E}\sum_n\frac{\mu^n}{n!}=\frac{0.50e^{\mu}}{E}=\frac{0.50E_0}{E^2}, \tag{32}$$

which is the same energy distribution as that given by Eq. (14). Thus, as was surmised in Sec. III, inclusion of the spatial variation of ψ has only a slight effect on the spectrum of secondary electrons.

VII

The energy distribution of secondary electrons is not the only quantity which gives direct information about the internal electron cascade in metals. The variation of total yield with work function also determines, to a considerable extent, the form of the internal energy distribution. This is so because the yield is proportional to the integral of the probability of escape [Eq. (27)] times the internal energy distribution [Eq. (26)] and thus depends on the shape of the latter. That is

$$\delta\sim\int^{\infty}E_F+\varphi l\frac{P(E)dE}{E^x}. \tag{33}$$

For the time being, the energy dependence of l will be neglected in accordance with the remark after Eq. (20). This expression can then be simplified by making use of the fact that P is a function of $(E/E_F+\varphi)$ and using this quantity as a new variable of integration. δ is then proportional to

$$\frac{1}{(E_F+\varphi)^{x-1}}\int_1^{\infty}P(y)\frac{dy}{y^x}, \tag{34}$$

if x is assumed constant. The integral is now independent of the work function and a simple differentiation gives the desired result,

$$\partial(\ln\delta)/d\varphi=\frac{1-x}{(E_F+\varphi)}. \tag{35}$$

This formula is correct to within about 10 percent in the range where $l(E)$ changes slowly.

Experimental measurements of the change in yield with work function have been made by a number of workers.[2] The technique used consists in covering the surface of a high work function metal (tungsten) with a thin layer of low work function material such as sodium. By varying the thickness of the Na layer (from zero to one monolayer) it is possible to obtain surfaces having work functions ranging from about 2.2 to 4.5 ev. In this method the amount of low work function metal deposited is exceedingly small so that the bulk properties

[12] John Weymouth, Phys. Rev. **84**, 766 (1951).

of the material are unchanged and the internal energy distributions remain typical of the high work function base. Under these conditions the only change in yield comes through the change in φ and should, therefore, be calculable from Eq. (35). Using for x its value at a point 2 ev above the vacuum level (estimated most probable velocity of secondaries), one obtains for tungsten the values:

$$\partial(\ln\delta)/\partial\varphi=-0.12 \text{ ev}^{-1} \quad \text{at} \quad \varphi=4.5 \text{ ev},$$

and

$$\partial(\ln\delta)/\partial\varphi=-0.14 \text{ ev}^{-1} \quad \text{at} \quad \varphi=3.5 \text{ ev}.$$

These numbers compare well with the experimental values of -0.12 and -0.15 ev^{-1}, respectively. At very low work functions the assumption $l(E)=$ constant is no longer valid so that Eq. (35) should not apply. In this range $l(E)$ increases rapidly as E approaches E_F. Just such behavior is evident in McKay's data where, below $\varphi=3$ ev, the value of δ increases much faster than it does for higher values of the work function. At 2.5 ev, for example, $\partial(\ln\delta)/\partial\varphi$ has reached about -0.5 ev^{-1}. A crude theoretical estimate, made by evaluating the integrand of Eq. (33) numerically for two adjacent values of the work function, gives $\partial(\ln\delta)/\partial\varphi=-0.35$ ev^{-1} at $\varphi=2.5$ ev, again in reasonably good accord with the observed value. Thus the theory of the internal electron cascade predicts in a fairly detailed way the course of the $\partial(\ln\delta)/\partial\varphi$ *versus* φ curve. As a matter of fact, the agreement is probably partly fortuitous since one would not expect a theory based on a free electron model to apply to a metal as complicated as tungsten. Nevertheless, it is evident that the change of work function with yield provides an important tool for investigating internal energy distributions and it is to be hoped that further experiments along this line will be carried out. In particular, it would be very useful to have measurements of $\partial(\ln\delta)/\partial\varphi$ for a metal to which one could apply the free electron model with real confidence in its validity.

VIII

The preceding sections of this paper have dealt with the problem of the shapes of electron energy distributions. In them no attempt was made to calculate the absolute yield of secondary electrons. Indeed, any such calculation is bound to be quite difficult since, as was pointed out in the introduction, it depends critically on both of the fundamental steps in the SE process. On the other hand, the mechanism proposed above to explain the SE spectra is a rather explicit one and it is important to know whether or not it is at least consistent with the observed values of total electron yield. In this section, therefore, an estimate will be made of the total yield which, though not good enough to give quantitative values of δ, will show that the picture of SE developed in the earlier part of this article is a reasonable one in this respect.

The total yield values are obtained by solving the transport equations [Eq. (30)] with a source function that takes account of the fact that primaries have only a finite depth of penetration into the metal. The simplest function which includes this finite range is

$$\begin{aligned} &S_0=A\delta(E-E_0), \quad (0<z<z_0), \\ &S_0=0, \qquad\qquad (z<0, z>z_0), \end{aligned} \tag{36}$$

where both z_0 and A are functions of the bombarding energy V_p. Even with this simple form for S_0, the complete solution of the equations is very difficult, but an asymptotic formula (for large z_0) can be obtained fairly readily and it will be used in subsequent calculations. The asymptotic form, which is derived in Appendix B, is

$$\psi_1(0,E)\cong\frac{AE_0}{2E^2}\left[1-\frac{40}{3\pi}\frac{l}{z_0}\right]. \tag{37}$$

The necessary value of A and the energy dependence of z_0 are obtained from Bohr's[13] formula for the rate of energy loss by fast electrons moving through matter. They are

$$A=\frac{\pi n_0 e^4}{V_p}\frac{1}{E_0^2}J_0, \tag{38}$$

and

$$z_0\sim V_p^2.$$

Here V_p is the bombarding energy, J_0 the primary current, and n_0 the number of electrons per cubic centimeter in the metal which are bound loosely enough to contribute to secondary emission. The total yield δ is now obtained by integrating over E and E_0. In calculating δ, the variation of $\sigma_{\text{eff}}(E)$ with energy, as well as the cut-off factor $P(E)$, will be neglected. The effects of these two factors are not large, and in addition they tend to cancel one another, so that for the crude sort of estimate being made here they can be dropped. The total secondary current is then

$$J_s=\frac{\pi n_0 e^4 J_0}{2n_c\sigma_{\text{eff}}V_p}\int\int\left[1-\frac{40}{3\pi}\frac{l_0}{z_0}\right]\frac{dE}{E^2}\frac{dE_0}{E_0}, \tag{39}$$

where n_c is the density of electrons in the conduction band and σ_{eff} an average value of the electron-electron cross section. The limits on the two integrations are $\varphi+E_F<E<E_0$ and $\varphi+E_F<E_0<V_p$. This assumes that the energy distribution is proportional to $1/E^2$ up to $E=V_P$. Actually, of course, the form of the distribution changes when E reaches W, but the contribution to the integral from electrons with $E>W$ is small, so the error made is not large. The result of the integration is

$$\delta=\frac{J_S}{J_0}=\frac{\pi n_0 e^4}{2n_c\sigma_{\text{eff}}V_P(\varphi+E_F)}\times\left[1-\frac{40}{3\pi}\frac{l_0}{z_0}\right]\left[\ln\left(\frac{V_P}{\varphi+E_F}\right)-1\right]. \tag{40}$$

[13] N. Bohr, Phil. Mag. **24**, 10 (1913).

This formula is most conveniently tested by maximizing δ and comparing the calculated $\delta_{\max}$ values with those obtained experimentally. Using the form given in Eq. (38) for the energy dependence of z_0 one obtains

$$\delta_{\max}=\frac{4}{3}\left(\frac{\pi a_0^2}{\sigma_{\text{eff}}}\right)\left(\frac{n_0}{n_c}\right)\frac{(Ry)^2}{(\varphi+E_F)V_P(\max)}\times\left[\ln\left(\frac{V_P(\max)}{\varphi+E_F}\right)-1\right], \quad (41)$$

where a_0 is the Bohr radius. In evaluating $\delta_{\max}$ the values of $V_P(\max)$ will be taken from experiment. In principle, of course, $V_P(\max)$ could also be calculated provided one knew the constant of proportionality in Eq. (38). However, with the somewhat oversimplified source function that is being used it is rather hard to know what value to choose for this constant. The present method avoids the difficulty by using only the energy dependence of z_0 in calculating $\delta_{\max}$.

Before using Eq. (41) to obtain $\delta_{\max}$ some method must be found for evaluating n_0/n_c. For low $V_P(\max)$ (Li, for example) n_0/n_c is equal to unity since all but the conduction electrons have a binding energy which is of the order of $V_P(\max)$ and hence cannot contribute appreciably to the SE. At higher bombarding energies the electrons in lower shells begin to play a role. An approximate idea of how important they are can be obtained by including a binding energy correction in the integral of Eq. (39). The effect of the binding is to move each internal electron cascade down in energy by just the binding energy. The integral then becomes

$$\int\int \frac{(E_0-E_B)}{E^2}\frac{dE_0dE}{E_0^2}, \quad (42)$$

where E_B is the binding energy and the limits now are $\varphi+E_F<E<E_0-E_B$ and $E_B<E_0<V_P$. The result of the integration is approximately

$$\frac{1}{(\varphi+E_F)}\left[\ln\left(\frac{V_P}{E_B}\right)-1\right], \quad (43)$$

whereas without the binding energy this term is

$$\frac{1}{(\varphi+E_F)}\left[\ln\left(\frac{V_P}{\varphi+E_F}\right)-1\right]. \quad (44)$$

TABLE II. Total yield values.

Element	$\delta_{\max}$(calc)	$\delta_{\max}$(obs)
Al	0.7	1.5
Cu	1.3	1.3
Li	0.6	0.5
Ag	1.1	1.5
K	1.3	0.7

Thus the effectiveness of the bound electrons is measured by the ratio:

$$\frac{\ln(V_P/E_B)-1}{\ln[V_P/(\varphi+E_F)]-1}. \quad (45)$$

The number of bound electrons in each shell will be multiplied by the appropriate factor of this type to obtain the effective number of electrons contributing to n_0. Tabulated in Table II[14] are $\delta_{\max}$ values obtained using this procedure. Considering the crudeness of the approximations used in deriving and evaluating Eq. (41) the agreement with experiment is satisfactory, indicating that the cascade theory of SE is at least consistent with the observed values of total yield.

In calculating the $\delta_{\max}$ values for Table II, σ_{eff} was taken equal to πa_0^2. Actually, in elements such as K or Na it should be considerably larger since the density of conduction electrons in these metals is quite low. Conversely, in Al or Be the correct values of σ_{eff} are probably somewhat lower than πa_0^2 since these metals have an especially high electron density. Inclusion of this effect would give better agreement between theory and experiment but, since really good values of $\delta_{\max}$ could only be obtained by a considerably more refined approach than that given above, it was not deemed worth while to perform the extra calculations necessary to incorporate it into the table.

IX

The theory presented in this article predicts the shapes of secondary electron spectra from monovalent metals by investigating the behavior of the electronic cascade process within the solid. The agreement with experiment that is obtained suggests that this is a valid and useful way of picturing the second stage of SE. Probably it could be applied with equal success to study SE from more complicated metals. However, in such cases the conduction and secondary electrons could no longer be treated as being free so that, before the cascade process could be investigated, one would have to understand how electron-electron scattering is modified by the presence of a strong crystal field.

In conclusion the author would like to express his indebtedness to Dr. K. G. McKay who, through a number of stimulating conversations, has contributed greatly to his insight into the whole problem of SE. He would also like to thank Conyers Herring for helpful comments and discussion on the topics discussed here.

APPENDIX A

Equations (30) of the text are most simply solved[15] by Laplace transforming with respect to z and Mellin transforming with respect to E. The result is the

[14] Experimental values here are the work of various authors. They are all taken from McKay's review article.

[15] The analysis culminating in Eq. (8a) is essentially the same as Weymouth's. For a more detailed exposition, see his paper.

following pair of algebraic equations:

$$\left(\frac{s-1}{s+1}\right)\psi_0(y,s)+yl_0\psi_1(y,s)=l_0\chi_1(s)+S_0(y,s),$$
$$\frac{yl_0}{3}\psi_0(y,s)+\left(\frac{s-\frac{1}{2}}{s+\frac{3}{2}}\right)\psi_1(y,s)=\frac{l_0}{3}\chi_0(s). \tag{1a}$$

Here

$$\psi_0(y,s)=\int_0^\infty dze^{-yz}\int_0^\infty dEE^s\psi_0(z,E),$$
$$\psi_1(y,s)=\int_0^\infty dze^{-yz}\int_0^\infty dEE^s\psi_1(z,E),$$
$$\chi_0(s)=\int_0^\infty dEE^s\psi_0(0,E), \tag{2a}$$
$$\chi_1(s)=\int_0^\infty dEE^s\psi_1(0,E),$$

and

$$S_0(y,s)=\int_0^\infty dze^{-yz}\int_0^\infty dEE^sS_0(z,E)=AE_0{}^s/y. \tag{3a}$$

The solutions of these algebraic equations are easily obtained; for example,

$$\psi_0=\begin{vmatrix} l_0\chi_1+S_0 & yl_0 \\ \frac{1}{3}l_0\chi_0 & (s-\frac{1}{2})/(s+\frac{3}{2}) \end{vmatrix} \Bigg/ \left[\frac{(s-1)(s-\frac{1}{2})}{(s+1)(s+\frac{3}{2})}-\tfrac{1}{3}l_0{}^2y^2\right]. \tag{4a}$$

In inverting the Laplace transforms to obtain $\psi(z,s)$, there are poles at

$$y=\pm\frac{\sqrt{3}}{l_0}\left(\frac{(s-1)(s-\frac{1}{2})}{(s+1)(s+\frac{3}{2})}\right)^{\frac{1}{2}}=y^{\pm}(s), \tag{5a}$$

one of which will give an exponentially rising solution, the other a decaying one, for large positive z. Since ψ_0 and ψ_1 must remain bounded as $z\to\infty$ one of the boundary conditions is that the coefficient of the positive exponential be zero, i.e.,

$$\begin{vmatrix} l_0\chi_1+AE_0{}^s/y^+(s) & l_0y^+(s) \\ \frac{1}{3}l_0\chi_0 & (s-\frac{1}{2})/(s+\frac{3}{2}) \end{vmatrix}=0. \tag{6a}$$

The other boundary condition is the requirement that there be no incoming current at the metal surface; that is,

$$\int_0^1 \chi_0\cos\theta d(\cos\theta)+\int_0^1 \chi_1 3\cos^2\theta d(\cos\theta)=0,$$

or

$$\tfrac{1}{2}\chi_0+\chi_1=0. \tag{7a}$$

These two equations may now be solved for χ_0, χ_1, which are the quantities needed since they determine the current at the surface. For instance,

$$\chi_1(s)=AE_0{}^s\left[\frac{3(s-1)(s-\frac{1}{2})}{(s+1)(s+\frac{3}{2})}\right]^{-\frac{1}{2}} \times\left\{1+\tfrac{2}{3}\left[\frac{3(s-1)(s+\frac{3}{2})}{(s+1)(s-\frac{1}{2})}\right]^{\frac{1}{2}}\right\}^{-1}. \tag{8a}$$

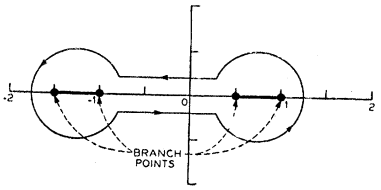

FIG. 6. Path of integration in complex plane.

The final step in the analysis is the inversion of this Mellin transform. To do this one must evaluate the integral

$$\frac{1}{2\pi i}\int_{\delta-i\infty}^{\delta+i\infty}\chi_1(s)E^{-(s+1)}ds =\frac{1}{2\pi i}\int_{\delta-i\infty}^{\delta+i\infty}\frac{1}{E}e^{s\mu}\left[\frac{3(s-1)(s-\frac{1}{2})}{(s+1)(s+\frac{3}{2})}\right]^{-\frac{1}{2}} \times\left\{1+\tfrac{2}{3}\left[\frac{3(s-1)(s+\frac{3}{2})}{(s-1)(s-\frac{1}{2}}\right]^{\frac{1}{2}}\right\}^{-1}ds \tag{9a}$$

where $\mu=\ln(E_0/E)$. The path of integration, which is parallel to the imaginary axis and to the right of all singularities, may be deformed to encircle the four branch points of $\chi_1(s)$ as shown in Fig. 6. With this contour s ranges only over finite values so that for small μ the inversion can be performed by expanding $e^{s\mu}$ into a power series and evaluating it term-by-term. The nth term in this series has the form

$$\frac{1}{2\pi i}\oint\frac{1}{E}\frac{(s\mu)^n}{n!}\left[\frac{3(s-1)(s-\frac{1}{2})}{(s+1)(s+\frac{3}{2})}\right]^{-\frac{1}{2}} \times\left\{1+\tfrac{2}{3}\left[\frac{3(s-1)(s+\frac{3}{2})}{(s+1)(s-\frac{1}{2})}\right]^{\frac{1}{2}}\right\}^{-1}ds, \tag{10a}$$

where the contour of integration is the loop in Fig. 6 which encircles all the singularities in the finite plane. For $s=\infty$ the integrand has a pole; hence the value of the integral can be obtained by replacing s by $1/q$ and calculating the residue at $q=0$. When n is big the evaluation of this residue is very tedious so that for large μ the method is not practical. Fortunately, however, for SE one is only interested in values of μ up to about 2 (a factor of 10 in energy). In this case only the first 4 or 5 terms in the series are necessary. Equation (9a) is then given by

$$\frac{1}{E}\left[0.54+0.48\mu+\frac{0.46}{2!}\mu^2+\frac{0.46}{3!}\mu^3+\frac{0.43}{4!}\mu^4+\cdots\right], \tag{11a}$$

which is just Eq. (31) of the text.

As was mentioned above, this series expansion method is not useful for large μ. In this case, though, the integrand in Eq. (9a) has a sharp minimum on the positive real s axis and the integral can be evaluated by saddle point integration. Calculations show that with the two methods it is feasible to perform the inversion for all values of μ from 0 to ∞.

APPENDIX B

With a finite range source [Eq. (33)] the transport equations can be solved by the same method used in Appendix A. As a matter of fact, Eq. (8a), when rewritten in terms of S_0, gives exactly the solution desired:

$$\chi_1(s)=\frac{S_0(y^+(s),s)}{l_0}\left\{1+\tfrac{2}{3}\left[\frac{3(s+1)(s+\frac{3}{2})}{(s+1)(s-\frac{1}{2})}\right]^{\frac{1}{2}}\right\}^{-1}. \quad (1b)$$

In the present case $S_0(y^+(s),s)$ is given by

$$S_0(y^+(s),s)=\frac{AE^s{}_0l_0\{1-\exp[-y^+(s)z_0]\}}{\sqrt{3}y^+(s)}. \quad (2b)$$

Without the $\exp[-y^+(s)z_0]$ term (1b) reduces to (8a) and can be inverted by the method given there. The part of the integral involving $\exp[-y^+(s)z_0]$ is much more complicated and will only be evaluated in the limit of large z_0. It is given by the expression

$$\frac{1}{2\pi i}\int_{\delta-i\infty}^{\delta+i\infty} \times\frac{A\exp\left\{\dfrac{-z_0}{l_0}\left[\dfrac{3(s-1)(s-\frac{1}{2})}{(s+1)(s+\frac{3}{2})}\right]^{\frac{1}{2}}\right\}\left(\dfrac{E_0}{E}\right)^s ds}{E\left[\dfrac{3(s-1)(s-\frac{1}{2})}{(s+1)(s+\frac{3}{2})}\right]^{\frac{1}{2}}\left\{1+\tfrac{2}{3}\left[\dfrac{3(s-1)(s+\frac{3}{2})}{(s+1)(s-\frac{1}{2})}\right]^{\frac{1}{2}}\right\}}. \quad (3b)$$

For large z_0 the exponent has a sharp maximum near $s=1$. Therefore, to obtain the first term in the asymptotic expansion set $s=1$ in all slowly varying terms. The result is that Eq. (3b) becomes

$$\sim\frac{1}{2\pi i}\int_{\delta-i\infty}^{\delta+i\infty}\frac{A}{E}\frac{1}{[3(s-1)/10]^{\frac{1}{2}}} \times\exp\left\{\frac{-z_0}{l_0}\left[\frac{3(s-1)}{10}\right]^{\frac{1}{2}}\right\}\frac{E_0}{E}ds. \quad (4b)$$

Now let $s-1=it$ and integrate up the line defined by $R(s)=1$ (going to the right of the branch point at $s=1$). Equation (4b) then breaks into two integrals:

$$\frac{1}{2\pi}\int_0^\infty\frac{A}{(3/20)^{\frac{1}{2}}(1+i)t}\exp\left[-\left(\frac{3}{20}\right)^{\frac{1}{2}}\frac{z_0}{l_0}(1+i)\sqrt{t}\right] \times\frac{E_0}{E^2}dt+\frac{1}{2\pi}\int_0^\infty\frac{A}{(3/20)^{\frac{1}{2}}(1+i)t} \times\exp\left[-\left(\frac{3}{20}\right)^{\frac{1}{2}}\frac{z_0}{l_0}(1-i)\sqrt{t}\right]\frac{E_0}{E^2}dt. \quad (5b)$$

The fact that $(1+i)$ appears in the first and $(1-i)$ in the second of these integrals is due to the fact that the two integrals refer to different branches of the square root. These integrals can now be rewritten as the sum of two real ones and it is a straightforward calculation to show that this first term in the asymptotic expansion is

$$(20/3\pi)(AE_0/E^2). \quad (6b)$$

Combining this with the calculation of Appendix A, one is led directly to Eq. (37) of the text.